


Submitted: October 30, 2023

Revised: November 7, 2023

Accepted: December 8, 2023

In-situ high-temperature bending strength measurement of YSZ ceramics manufactured using novel B₂O₃-based glass binder

P. Maniakin¹, S.G. Shalagaev², I.Yu. Archakov³ ,  Ya.V. Konakov^{1,3}, 

O.Yu. Kurapova^{3,4},  V.G. Konakov¹⁻³

¹Peter the Great St. Petersburg Polytechnic University, St. Petersburg, Russia

²Glass and Ceramics, LTD, St. Petersburg, Russia

³Institute for Problems in Mechanical Engineering RAS, St. Petersburg, Russia

⁴St. Petersburg State University, St. Petersburg, Russia

✉ ivan.archakov@gmail.com

ABSTRACT

Stabilized zirconia ceramics are in high demand for various high temperature applications as fuel cells, oxygen sensors or protective barriers in aircraft. The use of additive manufacturing with polymeric binders do not allow the application of manufactured zirconia ceramics units at high temperature. The present research highlights the manufacturing of cubic yttria stabilized zirconia (YSZ) using Co₃O₄-doped MgO-BaO-B₂O₃ glass as a novel high-temperature binder. In order to produce ceramics, YSZ powder with 4 wt. % of glass binder was milled in a planetary mill, compacted using isostatic cold pressing and annealed at 1500 °C for 2 hours. Sol-gel co-precipitated YSZ powder with average particle size of 290 nm was used as a precursor. The structure of ceramics was investigated via HR-SEM, EDS, XRD, hydrostatic weighting. In situ 3-point bending strength measurement showed that the ultimate bending strength is 104 ±10 MPa at room temperature. Temperature increase induces the linear decrease of bending strength value. Fractography tests revealed that the glass binder plays a key role in the mechanical behavior of the ceramics. The ways to improve the mechanical behavior of ceramics are suggested.

KEYWORDS

yttria stabilized zirconia • bending strength • glass binder • high temperature ceramics • in-situ measurements

Acknowledgements. This work was supported by Russian science foundation (RSF #23-19-00236). SEM and EDS data of the powders and consolidated ceramics as well as fracture of specimens after mechanical tests were obtained at the Research park of St. Petersburg State University "Interdisciplinary Center for Nanotechnology".

Citation: Maniakin P, Shalagaev SG, Archakov IYu, Konakov YaV, Kurapova OYu, Konakov VG. In-situ high-temperature bending strength measurement of YSZ ceramics manufactured using novel B₂O₃-based glass binder. *Materials Physics and Mechanics*. 2024;52(2): 64–75.

http://dx.doi.org/10.18149/MPM.5222024_7

Introduction

Due to a set of its unique characteristics, Yttria Stabilized Zirconia (YSZ) ceramics is considered as one of the most perspective materials of XXI century. Depending on the type of zirconia allotrope it is widely used in the various fields of modern industry: cubic zirconia is utilized in solid oxide fuel cells [1–5], high-temperature oxygen sensors [6,7], optical sensors [8], tetragonal zirconia is used as a biomaterial for dentistry and orthopedy [9,10], as thermal barriers coatings for aircraft [11], etc. The available literature data on the YSZ mechanical properties mainly concerns the behavior of the tetragonal phase of

zirconia or partially stabilized zirconia at room temperature or at presence of a moisture [9,12–15]. Paper by L. Zhou et al. [16] reports the properties of yttria-stabilized zirconia computed by molecular dynamics simulations depending on the crystal orientation. YSZ structure here was obtained by random replacement of Zr^{4+} in ZrO_2 by Y^{3+} ; in order to save the charge neutrality, one oxygen atom was removed for every two Zr^{4+} replacements. Rather high values of the Young's modulus (325-400 GPa at room temperature and ~ 325 GPa at 1000 °C) and Poisson's ratio (0.45 and 0.4 at 25 and 1000 °C, respectively) were obtained; note that the authors consider the temperature dependence of the mechanical properties to be rather low. Authors of [17] performed a set of computations for a wide range of zirconia-based objects: cubic, tetragonal and monoclinic ZrO_2 , pure cubic YSZ and cubic YSZ (c-YSZ) doped by some metal oxides; density functional theory was used for this task. In contrast to [16], the difference in the mechanical properties attributed to the different crystal orientation is considered to be quite significant: the strain strength in the [100] direction is ~ 2.8 times higher than in the [110] one. The high value of Young's modulus (277 GPa), bulk modulus (239 GPa), shear modulus (106 GPa) and Poisson's ratio of 0.307 at room temperature are reported for cubic YSZ. The experimental work [18] reports the study of the spark plasma sintered YSZ mechanical properties. It should be noted that the obtained ceramics was quite porous, the best porosity obtained at higher temperature and pressure values exceeds 10 % for tetragonal YSZ. The drastic porosity effect on the YSZ mechanical properties is discussed: as an example, Young's modulus at minimal porosity is ~ 170 GPa, while at a maximal one (40 %) it decreases down to ~5 GPa. Similar effect was also shown for the Vickers hardness (~ 1050 and ~ 200 $HV_{0.3}$, respectively) and for the flexural strength (~ 320 and ~ 40 MPa, respectively). YSZ (8 % yttria) Young's modulus as a function of temperature was studied by S. Giraud and J. Canel [19], ceramics here were synthesized from powders by cold pressing at 250 MPa with a further annealing at 1350 °C for 3 h in air. The following data were obtained for Young's modulus, modulus of rigidity and Poisson's ratio at room temperature: 205, 78 GPa and 0.31, respectively. The authors report the complicated Young's modulus dependence on the temperature: it slowly decreases in the temperature range up to 150 °C; this decrease is more evident at 150-550 °C. However, an increase in the Young's modulus value was observed at temperatures higher than 600 °C. Finally, rather high Young's modulus value is reported for the maximal temperature of 1000 °C – ~ 150 GPa. The work by T. Kushi et al. [20] deals with the temperature effect of the elastic modulus and the internal friction of YSZ itself ($Zr_{0.85}Y_{0.15}O_{1.93}$) and YSZ doped by a number of metal oxides; specimens under study were produced within the traditional ceramic approach (cold pressing at 150 MPa with further sintering at 1350 °C). The mechanical properties of the specimens were investigated in an oxidizing and a reducing atmosphere (O_2 and H_2 additions to Ar) in the temperature range from room to 1300 K. It was shown that the temperature behavior of the Young's modulus is similar to that reported in [19], the difference between the values typical for both atmospheres seems to be rather low. Young's modulus demonstrated some decrease from ~210 GPa at room temperature to ~ 160 GPa at 1023 °C; the decrease in the shear modulus was not so distinctive (~ 75 and 55 GPa, respectively), while the Poisson's ratio was not linear and demonstrated some increase from ~ 0.38 to ~ 0.4. A recent paper [21] discusses the yttria contents effect of on the YSZ microstructure and mechanical

properties. A conventional approach (sintering at 1550 °C for 2 h in argon) was used to prepare the specimens, it should be noted that the obtained specimens were the mixture of monoclinic, tetragonal, and cubic phases. The flexural strength of the studied materials varied from 900 to 500 MPa depending on the yttria contents, the highest values were obtained for the compositions with 3, 7, and 8 % of yttria. The authors stated that the variations in the flexural strength value coincide with the variations in the monoclinic phase contents. The work by X. Ren and W. Pan [22] considers the changes in the mechanical properties of 8 wt. % yttria-stabilized zirconia ceramics due to the thermal degradation of the metastable tetragonal phase. The specimens for the study were manufactured using the powder air spraying to obtain metastable T' phase powders which were then ball milled and sintered at 1450 °C for 5 min under a unidirectional pressure of 50 MPa by the SPS method. Note that the samples cut for the mechanical testing were additionally hardened by an annealing at 1300 °C for 1–24 h. The authors report the following typical values for the samples depending on the metastable phase contents: Vickers hardness in the range from 13 to 14 GPa, elastic modulus of ~ 229 GPa, bending strength from 220 to 500 MPa, and fracture toughness from 4.0 to 5.4 MPa m^{1/2}. The effect of carbon nanotubes on the YSZ (3 % yttria) mechanical properties was investigated in [23], SPS approach (60 MPa with a maximum sintering temperature of 1450 °C) was used for the specimens production. The Young's modulus of ~ 290 GPa, the shear modulus of ~ 215 GPa, and the fracture toughness value of 4.1 MPa m^{1/2} were reported for the pure 3YSZ samples at room temperature. The effect of the phase composition is discussed. The effect of the thermal cycling on the mechanical properties of the tetragonal polycrystalline YSZ is reported in [24]. Rather high flexural strength value of 776 MPa is stated. The obtained values of the Young's modulus demonstrated an evident decrease with temperature from 206 GPa at room temperature to ~ 165 GPa at 850 °C, the thermal cycling seems to produce fairly low effect on the Young's modulus temperature behavior.

In summary, it can be stated that YSZ itself possesses rather high values of Young's and shear moduli, along with the bending (flexural) strength values. However, the mechanical properties of the exact specimen are highly affected by a lot of material characteristics: yttria contents, phase composition, synthesis approach, porosity, grain size, thermal prehistory, etc.

One of the main problems, hindering the comfortable YSZ usage, is the well-known difficulties dealing with manufacturing of the complex geometry pieces within the traditional ceramic approaches. Despite the traditional approaches to allow the fabrication of YSZ ceramics, they are often not cost-effective and often require the use of the additional machining tools. Additive technologies providing the automated production of the pieces with a precision geometry seems to be the evident decision of this problem; it is especially effective for the units with a highly developed system of internal surfaces – channels and cavities [12,25]. However, the use of the additive technologies for the production of ceramic units is characterized by a number of serious limitations, the detailed analysis of such limitations can be found in our recent work, see e.g. [26].

Modern approaches of the YSZ ceramic pieces production via additive manufacturing include stereolithography, ink jet-printing, tape casting, selective laser sintering (SLS), and selective laser melting (SLM) [25]. They are usually based on the use of organic or inorganic binders. Typically, organic binders are rather universal for all

ceramic materials including YSZ, asphotoreactive organic mixture provided by 3D CERAM Sinto, France [12], various acrylate derivatives, as 1,6-hexanediol diacrylate (HDDA) [27], 2-hydroxyethyl methacrylate (HEMA) [28] or polyvinylpyrrolidone (PVP) binder. Regretfully, the exploitation of the materials with such binders is usually restricted by temperatures below 250-300 °C. In turn, such inorganic colloid binders as TiO_2 [29], Ti_3SiC_2 , CoAl_2O_4 and ZrO_2 [30] provide higher exploitation temperatures. In [30], a zirconium basic carbonate was used as a binder to print zirconia based ceramic parts. Aqueoustetragonal zirconia-based inks with solid contents of 22 and 27 vol. % were used in [31] to fabricate three-dimensional ceramic parts by the ink-jet printing. The sintered ceramics reached up to ~ 97 % of the theoretical density. In both works, the focus was made on the rheological properties of slurries. The effects of the structure, sintering parameters on bending strength, compressive strength, and pore structure architecture were not studied. It should be noted that to produce the part having high mechanical properties, the binder should be matched with the ceramic matrix material according to the Coefficient of Thermal Expansion (CTE) [32]. The use of the glass binder with the same CTE as zirconia is prospective as such matching prevents the material destruction upon heating. Thus, the present work aims he the possibility of the use of Cobalt oxide-doped $\text{MgO-BaO-B}_2\text{O}_3$ glass (here and after Co-MBB glass) as a binder for the production of YSZ matrix pieces by additive technologies. Model specimens produced using the traditional ceramic approach were used for in-situ evaluation of the high-temperature bending strength of such a material. The result obtained is the decisive for the whole complex of further research – the possibility of the significant increase of the material exploitation temperature range is shown comparing with 250-300 °C limit typical for the materials produced using organic binders.

Methods

YSZ powders synthesis

The synthesis of $9\text{Y}_2\text{O}_3\text{-}91\text{ZrO}_2$ (YSZ) powders with the mean particle size of 290 nm was carried out using the co-precipitation approach followed by freeze-drying described in details in [33,34]. Yttrium and zirconyl nitrates hydrates $\text{Y}(\text{NO}_3)_3 \cdot 6\text{H}_2\text{O}$ (Acros organics, Geel, Belgium, 99.9 %) and $\text{ZrO}(\text{NO}_3)_2 \cdot 6\text{H}_2\text{O}$ (Acros organics, Geel, Belgium, 99.5 %) were utilized to prepare a 0.1 M aqueous mixed salt solution. A resulted salt solution was added dropwise to 1 M aqueous ammonia solution (LenReactiv Ltd, St. Petersburg, Russia, c.p.) at a rate of ~1–2 mL/min. The precipitation was performed at ~1–2 °C in an ice bath; the pH of the solution was controlled to be ~ 9–10 during the synthesis. To remove reaction byproducts, the obtained gel was filtered and rinsed by distilled water until the neutral pH was reached. The precipitate of mixed hydroxides was then freeze-dried (Labconco, 1L-chamber, Kansas City, MO, USA; 20 °C, 24 h, P = 0.018 mm Hg). The obtained powder was annealed at 650 °C for 3 hours, and then it was milled in a planerary mill (400 rpm, 12 reverse cycles of 5 minutes each, Pulverisette 6, Fritsch, Germany).

Co-MBB glass

A glass with 30MgO-35BaO-35B₂O₃ (mol.%) composition (further, MBB glass) was produced as follows: the starting reagents MgO, Ba(OH)₂×8H₂O, and H₃BO₃ (all LenReactiv Ltd, St. Petersburg, Russia, 99.98 %) were mixed in the required proportions; the mixture was ground in a porcelain mortar to a homogeneous powder (typical particle mean size ~ 15-25 μm, maximal < 40 μm). The obtained powder was kept in an alundum crucible at 1100 °C for about ~ 3 hours until the end of the gases release. The temperature was then increased up to 1250 °C, the glass was exposed at that temperature for 1.5 hours and then poured on a steel plate. As it was shown in [35], CTE of such glass in the temperature range from room to 1000 °C is close to that of YSZ [32]. Unfortunately, the obtained glass was fairly colorless and transparent making it quite inefficient as a binder in additive manufacturing, as Selective Laser Synthesis and Selective Laser Melting (SLS and SLM) approaches. To overcome this problem, MBB glass was doped by cobalt oxide Co₃O₄ as follows. Commercially available Co₃O₄ powder (mean size 18 μm, maximal particle size < 40 μm) was added to MBB glass powder in the ratio 100 g MBB glass powder / 4 g Co₃O₄ powder, the resulting powder was thoroughly mixed, the technology of glass baking was the same. The resulting glass has an evident blue color (Fig. 1) making it suitable for SLS / SLM approaches. At that, the relatively small addition of the cobalt oxide should not noticeably change the glass CTE.

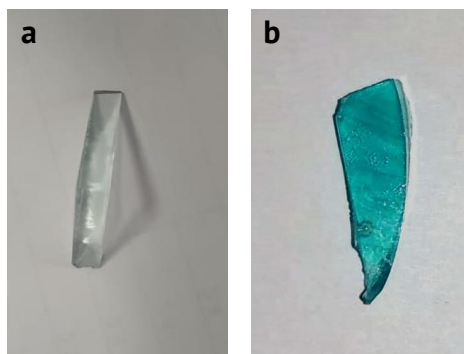


Fig. 1. Comparison of MBB glass (a) and Co-doped MBB glass (b)

In order to use the manufactured Co-MBB glass as a binder for ceramics manufacturing, the obtained material was crushed into powder using mortar and pestle. The high resolution scanning electron microscopy (HR-SEM) photos obtained in the scattered electron (SE) mode and back-scattered electron (BSE) mode of the resulted powder for a better contrast are presented in Fig. 2.

As seen, glass powder after crushing consists of the coarse particles with the sizes up to ~ 200 μm. However, due to the fragility of glass, individual particles of 10-20 μm are also present in the powder (see Fig. 2(b)). The BSE mode allows better phase contrast. The typical particles are non-porous with the glassy-like fracture surface. The use of the MBB powder as a binder requires additional milling in a planetary mill. According to the EDS spectra obtained for the glass powder, the chemical composition of obtained glass corresponds to the MgO:BaO = 1.28 and differs from the initial mixture. Surely, long-term annealing is accompanied by the change of the glass binder composition due to intensive Ba(BO₂)₂ evaporation, more heat resistive composition enriched by MgO is formed.

However, estimates of the composition changes according to [36] indicate the minor effect of low-volatile components evaporation in the discussed case.

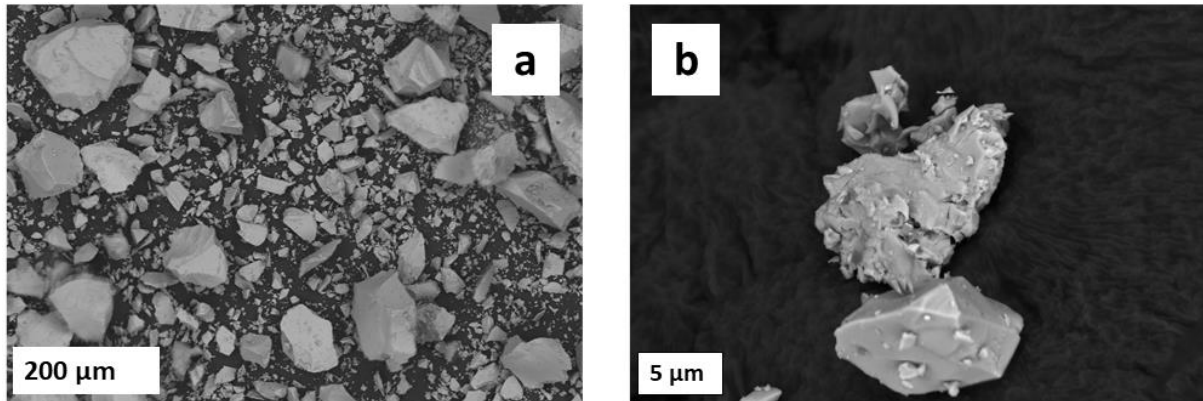


Fig. 2. HR-SEM photos of powdered Co-MBB glass: (a) SE mode, magnification \times 200, (b) magnification \times 5000

YSZ ceramics manufacturing

YSZ and Co-MBB glass powders taken in a ratio of 95 and 4 wt. %, respectively, were mixed in Pulverisette 6 planetary ball mill (250 rpm for 1 hour), placed in a steel press form (\varnothing 50 mm, height \sim 15 mm) and subjected to isostatic cold pressuring (15 tons/cm² for 20 min). Resulting disks were loaded on a corundum wafer and annealed at 1500 °C for 2 hours. After cooling to room temperature, specimens for bending strength tests (4 \times 5 \times 45 mm beams) were cut using Isomet 4000 precision saw. The final specimen preparation step was the final material hardening by annealing at 1400 °C for 2 hours.

Structure measurements

The phase composition of powders and ceramics after the synthesis and consolidation was investigated by X-Ray diffraction analysis (XRD). The XRD patterns were registered using SHIMADZU XRD-6000 ($\text{CuK}\alpha=1.54 \text{ \AA}$, $2\theta=10-80^\circ$, scan speed $0.02^\circ/\text{min}$), reflexes identification was carried out using PDF-2 database (release 2021). Microstructures and the chemical compositions of glass binder powder and polished ceramics were analyzed using high resolution scanning electron microscopy (HR-SEM, Zeiss Merlin, accelerating voltage 20 eV, equipped by a console for Energy-dispersive X-ray spectroscopy, EDS). Fracture surfaces of the ceramic samples after the bending tests were also analyzed in HR-SEM (Zeiss Merlin, accelerating voltage 20 eV). Apparent density of YSZ ceramics and ceramics after the mechanical tests at 19 and 1127 °C was measured by hydrostatic weighting technique (scales RADWAG 220 c/xc, Poland). Each sample was measured in the air and then in octane. The results were averaged for 3 parallel measurements of each sample. The theoretical density of material was calculated using the rule of mixtures. The theoretical density of the cubic YSZ ceramics was taken from crystallography data to be 5.96 g/cm³ [37] and MBBO density to be 3.67 g/cm³ [35].

In-situ 3-point bending strength measurements at high temperatures

In-situ estimation of 3-point bending strength at high temperatures was carried out as follows. We used a laboratory homemade setup based on the principles recommended by ISO 5014:1997 (Dense and insulating shaped refractory products, Determination of modulus of rupture at ambient temperature). The recommended 3-point scheme (supports – fused silicon carbide, load – tantalum rod) was realized inside the induction heated graphite cylinder, the temperature was measured by WR5-WR20 thermocouple placed directly on one of the supports, the measurement accuracy was ± 2 °C. The applied load was measured using Megeon 4500 dynamometer placed in a cold zone, the measurement accuracy was ± 1 %. Note that the working volume of the measuring cell during the high temperature measurements was filled by an inert gas (Ar, 99.99 wt. %) to prevent the graphite cylinder and metallic pieces of the measuring cell (Ta, Mo) oxidation. The data was averaged for 5 samples.

Results and Discussion

Typical XRD patterns for the ceramics after sintering at 1500 °C for 2 hours and after the bending strength tests at 1100°C are presented in Fig. 3.

As seen from Fig. 3, YSZ ceramics after sintering corresponds to the high crystalline single phase cubic solid solution with no admixtures of the other phases. All reflexes in the XRD pattern corresponds to cubic fluorite-like structure (space group $Fm\bar{3}m$, point group 225).

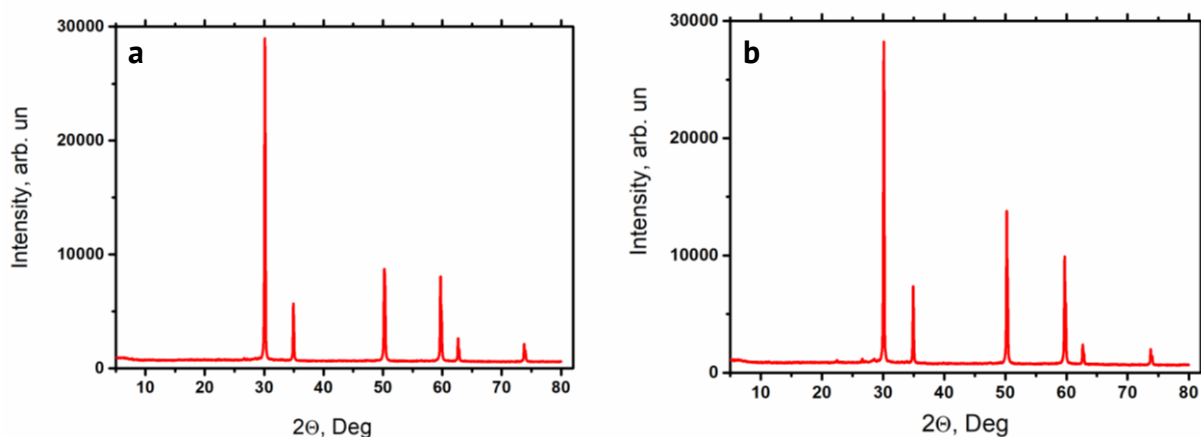


Fig. 3. XRD patterns obtained for the ceramics after sintering (a) and after bending strength tests at 1115 °C (b)

The microstructure of ceramics after sintering with Co-MMB glass binder and EDS elemental maps of Zr, Mg, Ba and O are presented in Fig. 4. Overall structure of ceramics contains some voids and pores, it is in accordance with the relative density of ceramics after sintering, being of 81.80 ± 0.11 %. The structure of the ceramics consists of well-defined grains with the typical sizes from 10 to 40 μm divided by rather thick grain boundaries (see Fig. 4(a)). Under higher magnification using the BSE mode for better phase contrast, one can see that a typical grain boundary is filled up by a transparent glassy phase. (see Fig. 4(b)). The ceramic grains are bonded together with the glassy wires.

The EDS mapping taken from the polished surface of ceramics (Figs. 4(b,c,f)) shows that zirconium is located only in the ceramics grains, whereas oxygen element is spread

between grains and grain boundaries and concentrated in the grain boundaries. Such elements as Mg and Ba are also located in grain boundaries only, corresponding to the Co-MBB glass (Figs. 4(b,c,f)). It should be noted that B is too light element to be detected by EDS, while the Co contents is too low to be detected.

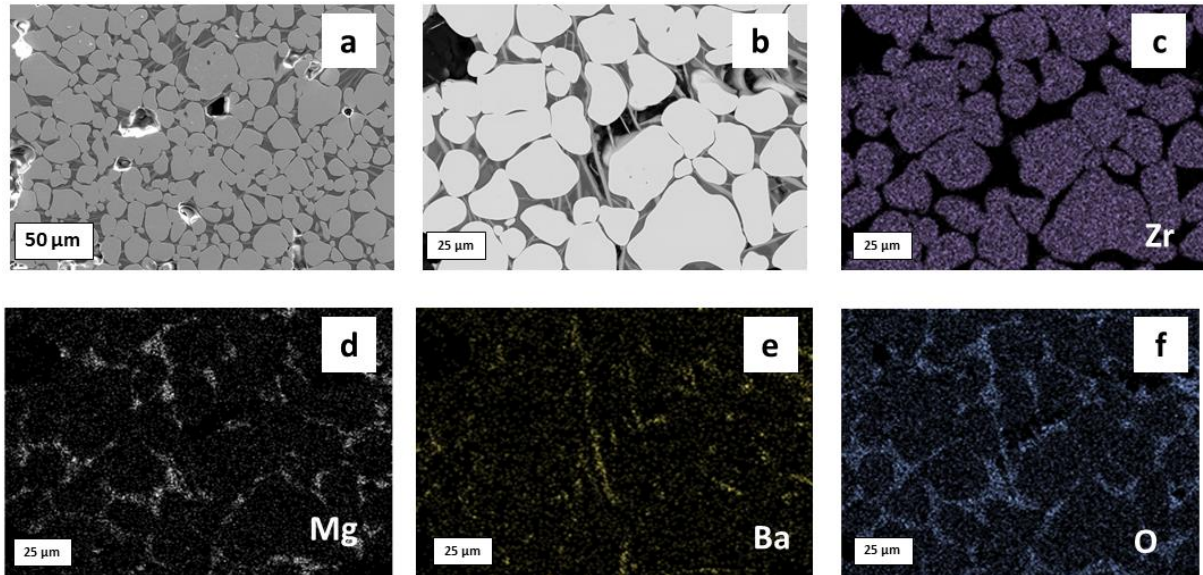


Fig. 4. HR-SEM images of (a) and (b) ceramics after sintering with Co-MBB glass binder, (c) EDS map of Zr, (d) EDS map of Mg, (e) EDS map of Ba, and (f) EDS map of O taken from HR-SEM image

Figure 5 presents the results of the bending stress tests, the temperature scheme of the test was as follows. First, reference values were obtained at room temperature (25 °C), they were compared with the data at 1000 °C. Measurements at intermediate temperatures (600 and 800 °C) provide an opportunity to understand the type of the bending strength vs temperature dependence. At the final step, the temperature was increased up to the value of the specimen break under the weight of the dynamometer without any additional load application.

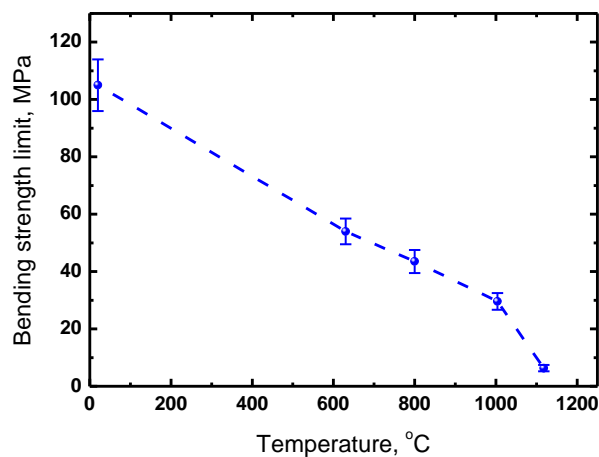


Fig. 5. Temperature dependence of the bending strength of YSZ ceramics with Co-MBB binder

As seen from the figure, the initial ultimate bending strength of the YSZ specimens studied (> 100 MPa) is typical for cubic yttria stabilized zirconia ceramics [6,38]. The evident decrease (~ 3 times) in the bending strength limit value is seen for the temperature of 1000 °C. Accounting for the data taken in the intermediate points, one could assume the linear character of the dependence. The break of the specimens under the dynamometer weight without any additional load application occurred at temperatures ~ 1115 °C.

A set of experiments was carried out to understand the above material behavior. First, the phase composition of the specimen after bending tests at high temperature was studied by XRD (Fig. 3(b)). The results, presented in Fig. 3(b), demonstrate the constancy of the YSZ matrix phase composition: the position of the reflexes obtained for the initial specimen (Fig. 3(a)) are the same as those for specimen tested at 1115 °C (Fig. 3(b)). In-situ bending test induces a slight change of the intensity of the reflexes at $2\theta = 51$ and 59° in the XRD pattern for ceramics. That is likely due to the texturing of ceramics exposed to in situ 3-point bending test at high temperature. HR-SEM and fractography analysis were performed to understand the state of the glass binder phase and to characterize the nature of the specimens fracture (see Fig. 6).

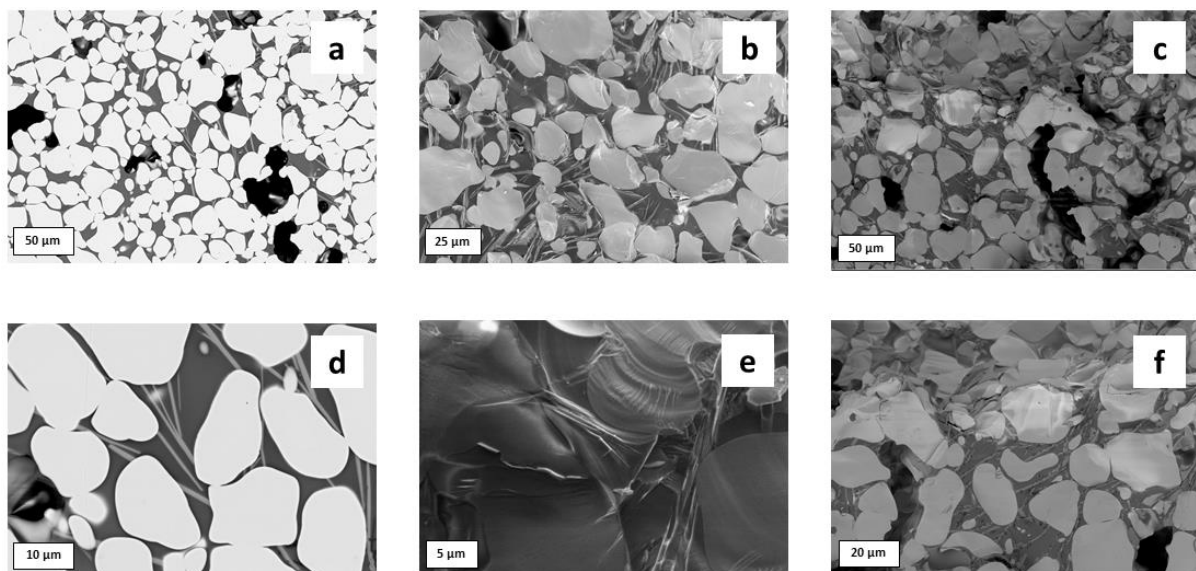


Fig. 6. HR-SEM images of (a) and (d) polished cross-section of ceramics with Co-MMB glass binder after fracture at 1115 °C in BSE mode; (b) and (e) cleavage surfaces for ceramics after mechanical tests at room temperature, SE mode (c) and (f) cleavage surfaces for ceramics after mechanical tests at 1115 °C, SE mode

The structure of YSZ ceramics after mechanical tests at 1115 °C remains unchanged (see Fig. 6(a,d)). The relative density of ceramics increases slightly up to 86.10 ± 0.07 %. The results of the fractography tests are of particular interest. Analyzing the above data, one can consider that the specimen's breakage is related to the Co-MBB glass binder state. Indeed, all cleavage surfaces are characterized by the glass binder presence and drastically differ from those typically observed for YSZ ceramics. An amorphous fracture is observed both at room and at high temperature. Upon the temperature increase, glass binder plays a key role in the bending strength decrease. Glass softening induces twice decrease in bending strength at 600 °C and its melting cause the bending strength values

drop almost to zero at 1115 °C. Indeed, according to the data on MgO-BaO-B₂O₃ phase diagram [23], the melting temperature for the compositions similar to MBB glass composition should be ~ 1170-1200 °C, similar value can be expected for the Co-MBB glass due to small amount of the cobalt oxide additive. It is worth noticing that amorphous fracture also takes place for ceramic grain. It may indicate that longer sintering time is necessary to achieve better formed structure.

In summary, the use of novel Co-MBB glass based inorganic binder is with no doubts prospective since it would allow increasing the temperature range of exploitation of the additively manufactured YSZ ceramics compared to the existing data on organic binder used for zirconia ceramics production via AM. The results obtained can be concerned as a basis for further comprehensive research including the optimization of the annealing and quenching temperatures and duration to eliminate binder predomination in the fracture; determination of the CTE of Co-MBB glass, manufacturing of YSZ ceramics via SLS and the detailed study of the structures and mechanical characteristics of such ceramics.

Conclusions

Using XRD it was shown that YSZ ceramics with the glass binder corresponds to a single phased cubic fluorite-like zirconia solid solution. Using HR-SEM and EDS mapping it was confirmed that the structure of ceramics consists of micron-sized grains separated by the thick grain boundaries filled up with the glassy binder. The relative density of ceramics increases from 81.80 ± 0.11 to 86.10 ± 0.07 % upon the testing temperature increase from room to 1115 °C with no change in the phase composition of ceramics. In-situ 3-point bending strength showed that the temperature increase induces the linear decrease of bending strength value from 104 ± 10 to 31 ± 3 MPa. Fractography tests revealed that amorphous fracture takes place at all temperature range studied, and the glass binder plays predominant role in the mechanical behavior of ceramics.

References

1. Carrette L, Friedrich KA, Stimming U. Fuel Cells: Principles, Types, Fuels, and Applications. *Chem Phys Chem*. 2000;1(4): 162–193.
2. Mahato N, Banerjee A, Gupta A, Omar Sh, Balani K. Progress in Material Selection for Solid Oxide Fuel Cell Technology: a Review. *Prog. Mater. Sci*. 2015;72: 141–337.
3. Kim J, Kim J, Yoon KJ, Son JW, Lee JH, Lee JH, Lee HW. Solid Oxide Fuel Cells with Zirconia/Ceria Bilayer Electrolytes via Roll Calendering Process. *J. Alloys Compd*. 2020;846: 156318.
4. Pesce A, Hornés A, Núñez M, Morata A, Torrella A, Tarancón A. 3D Printing the Next Generation of Enhanced Solid Oxide Fuel and Electrolysis Cells. *J. Mater. Chem. A*. 2020;8: 16926–16932.
5. Minh NQ. Ceramic Fuel Cells. *J. Amer. Ceram. Soc*. 1993;76(3): 563–588.
6. Terauchi S, Takizawa H, Endo T, Uchida S, Terui T, Shimada M. High Ionic Conductivity and High Fracture Strength of Cubic Zirconia, (Y_{0.16} – xSc_x)Zr_{0.84}O_{1.92}/Alumina Composites. *Mater. Lett*. 1995;23(4–6): 273–275.
7. Kurapova OYu, Pivovarov MM, Nikiforova KV, Konakov VG. Sensor Properties of Stabilized Zirconia Ceramics, Manufactured from Nanopowders. *Rev. Adv. Mater. Sci*. 2018;57(2): 257–261.
8. Sikarwar S, Yadav BC, Singh S, Dzhardimalieva GI, Pomogailo SI, Golubeva ND, Pomogailo AD. Fabrication of Nanostructured Yttria Stabilized Zirconia Multilayered Films and their Optical Humidity Sensing Capabilities Based on Transmission. *Sens Actuators B Chem*. 2016;232: 283–291.
9. Roitero E, Reveron H, Gremillard L, Garnier V, Ritzberger C, Chevalier J. Ultra-Fine Yttria-Stabilized Zirconia for Dental Applications: A Step Forward in the Quest Towards Strong, Translucent and Aging Resistant Dental Restorations. *J Eur Ceram Soc*. 2023;43(7): 2852–2863.

10. Khajavi P, Xu Y, Frandsen HL, Chevalier J, Gremillard R, Kiebach R, Hendriksen PV. Tetragonal Phase Stability Maps of Ceria-Yttria Co-Doped Zirconia: From Powders to Sintered Ceramics. *Ceram Int*. 2020;46(7): 9396–9405.
11. Pakseresht A, Sharifianjazi F, Esmaeilkhanian A, Bazli L, Nafchi MR, Bazli M, Kirubakaran K. Failure Mechanisms and Structure Tailoring of YSZ and New Candidates for Thermal Barrier Coatings: A Systematic Review. *Mater Des*. 2022;222: 111044.
12. Fournier S, Chevalier J, Baeza GP, Chaput Ch, Louradour E, Sainsot Ph, Cavoret J, Reveron H. Ceria-Stabilized Zirconia-Based Composites Printed by Stereolithography: Impact of the Processing Method on the Ductile Behaviour and its Transformation Features. *J Eur Ceram Soc*. 2023;43(7): 2894–2906.
13. Chevalier J, Loh J, Gremillard L, Meille S, Adolfson E. Low-Temperature Degradation in Zirconia with a Porous Surface. *Acta Biomater*. 2011;7(7): 2986–2993.
14. Chevalier J. What Future for Zirconia as a Biomaterial? *Biomaterials*. 2006;27(4): 535–543.
15. Chevalier J, Gremillard L, Virkar AV, Clarke DR. The Tetragonal-Monoclinic Transformation in Zirconia: Lessons Learned and Future Trends. *J. Amer. Ceram. Soc*. 2009;92(9): 1901–1920.
16. Zhou J, Zhang J, Zhong Z. Mechanical Properties of Yttria-Stabilized Zirconia: A Study by ReaxFF Molecular Dynamics Simulations. *Mechanics of Materials*. 2020;149: 103542.
17. Cousland GP, Cui XY, Smith AE, Stampfl APJ, Stampfl CM. Mechanical Properties of Zirconia, Doped and Undoped Yttria-Stabilized Cubic Zirconia from First-Principles. *J. Phys. Chem. Solids*. 2018;122: 51–71.
18. Fregeac A, Ansart F, Selezneff S, Estournès C. Relationship Between Mechanical Properties and Microstructure of Yttria Stabilized Zirconia Ceramics Densified by Spark Plasma Sintering. *Ceram Int*. 2019;45(17): 23740–23749.
19. Giraud S, Canel J. Young's Modulus of Some SOFCs Materials as a Function of Temperature. *J. Eur. Ceram. Soc*. 2008;28(1): 77–83.
20. Kushi T, Sato K, Unemoto A, Hashimoto Sh, Amezawa K, Kawada T. Elastic Modulus and Internal Friction of SOFC Electrolytes at High Temperatures under Controlled Atmospheres. *J. Power Sources*. 2011;196(19): 7989–7993.
21. Kulyk V, Duriagina Z, Kostryzhev A, Vasylyv B, Vavrukh V, Marenych O. The Effect of Yttria Content on Microstructure, Strength, and Fracture Behavior of Yttria-Stabilized Zirconia. *Materials*. 2022; 15(15): 5212.
22. Ren X, Pan W. Mechanical Properties of High-Temperature-Degraded Yttria-Stabilized Zirconia. *Acta Mater*. 2014;69: 397–406.
23. Jang BK, Lee JH, Fisher CAJ. Mechanical Properties and Phase-Transformation Behavior of Carbon Nanotube-Reinforced Yttria-Stabilized Zirconia Composites. *Ceram. Int*. 2021;47(24): 35287–35293.
24. Zhang J. Thermal Cycling Effect on Mechanical Properties of Yttria-Stabilized Tetragonal Zirconia. *Key Eng Mater*. 2013;538: 121–124.
25. Zhang X, Wu X, Shi J. Additive Manufacturing of Zirconia Ceramics: a State-of-the-Art Review. *J Mat. Res. Tech*. 2020;9(4): 9029–9048.
26. Golubev SN, Kurapova OYu, Archakov IYu, Konakov VG. Characterization of a High Temperature Ceramics Produced via Two-Step Additive Manufacturing. *Open Ceramics*. 2021;7: 100165.
27. Wang L, Yu H, Hao Z, Tang W, Dou R. Investigating the Effect of Solid Loading on Microstructure, Mechanical Properties, and Translucency of Highly Translucent Zirconia Ceramics Prepared via Stereolithography-Based Additive Manufacturing. *J. Mech. Behav. Biomed. Mater*. 2023;144: 105952.
28. Shao H, Zhao D, Lin T, He J, Wu J. 3D Gel-Printing of Zirconia Ceramic Parts. *Ceram Int*. 2017;43(16): 13938–13942.
29. Kuscer D, Stavber G., Trefalt G, Kosec M. Formulation of an Aqueous Titania Suspension and its Patterning with Ink-Jet Printing Technology. *J. Amer. Ceram. Soc*. 2012;95(2): 487–493.
30. Huang S, Huang S, Ye Ch, Zhao H, Fan Z, Wei Q. Binder Jetting Yttria Stabilized Zirconia Ceramic with Inorganic Colloid as a Binder. *Advances in Applied Ceramics*. 2019;118(8): 458–465.
31. Özkol E. Rheological Characterization of Aqueous 3Y-TZP Inks Optimized for Direct Thermal Ink-Jet Printing of Ceramic Components. *J Amer Ceram Soc*. 2013;96(4): 1124–1130.
32. Hayashi H, Saitou T, Maruyama N, Inaba H, Kawamura K, Mori M. Thermal Expansion Coefficient of Yttria Stabilized Zirconia for Various Yttria Contents. *Solid State Ion*. 2005;176(5–6): 613–619.
33. Kurapova OY, Glumov OV, Lomakin IV, Golubev SN, Pivovarov MM, Krivolapova JV, Konakov VG. Microstructure, Conductivity and Mechanical Properties of Calcia Stabilized Zirconia Ceramics Obtained from Nanosized Precursor and Reduced Graphene Oxide Doped Precursor Powders. *Ceram. Int*. 2018;44(13): 15464–15471.
34. Kurapova OY, Konakov VG. Phase Evolution in Zirconia Based Systems. *Rev. Adv. Mater. Sci*. 2014;36(2): 177–190.
35. Fomenko G, Nosenko A, Goleus V, Ilchenko N, Amelina A. Glass Formation and Properties of Glasses in Mgo-Bao-B₂O₃ System. *Chemistry & Chemical Technology*. 2015;9(4): 463–466.
36. Archakov IYu. *Evaporation of Borosilicate Glasses*. PhD Thesis. Institute for Silicate Chemistry RAS; 1993. (In Russian)

37. Glukharev A, Glumov O, Temnikova M, Shamshirgar AS, Kurapova O, Hussainova I, Konakov V. YSZ-rGO Composite Ceramics by Spark Plasma Sintering: The Relation Between Thermal Evolution of Conductivity, Microstructure and Phase Stability. *Electrochim. Acta*. 2021;367: 137533.
38. Abraham I, Gritzner G. Mechanical Properties of Doped Cubic Zirconia Ceramics. *J. Mat. Sci Lett*. 1993;12: 995–997.

About Authors

Peter Maniakin

Bachelor Student (Peter the Great St. Petersburg Polytechnic University, St. Petersburg, Russia)

Sergei G. Shalagaev

Engineer (Glass and Ceramics, LTD, St. Petersburg, Russia)

Ivan Yu. Archakov Sc

Candidate of Chemical Sciences

Senior Reseahcer (Institute for Problems of Mechanical Engineering RAS, St. Petersburg, Russia)

Yaroslav V. Konakov Sc

Junior Reseahcer (Peter the Great St. Petersburg Polytechnic University, St. Petersburg, Russia),

Researcher (Institute for Problems in Mechanical Engineering RAS, St. Petersburg, Russia)

Olga Yu. Kurapova Sc

Candidate of Chemical Sciences

Associate Professor (St. Petersburg State University, St. Petersburg, Russia),

Senior Researcher (Institute for Problems in Mechanical Engineering RAS, St. Petersburg, Russia)

Vladimir G. Konakov Sc

Doctor of Chemical Sciences

Professor (Peter the Great St. Petersburg Polytechnic University, St. Petersburg, Russia),

General Director (Glass and Ceramics, LTD, St. Petersburg, Russia),

Senior Researcher (Institute for Problems in Mechanical Engineering RAS, St. Petersburg, Russia)